BEFIB2012 – Fibre reinforced concrete
Joaquim Barros et al. (Eds)
 UM, Guimarães, 2012

FIBRE REINFORCED SELF-COMPACTING CONCRETE FLOW SIMULATIONS IN COMPARISON WITH L-BOX EXPERIMENTS USING CARBOPOL

Oldrich Svec[*], Jan Skocek[*], John Forbes Olesen[*] and Henrik Stang[*]

[*] Technical University of Denmark, Department of Civil Engineering
Brovej building 118 – 2800 Kgs. Lyngby, Denmark
e-mail: byg@byg.dtu.dk, web page: http://www.byg.dtu.dk

Keywords: Flow simulation, Lattice Boltzmann, Carbopol, fibres.

Summary: *An evolution of distribution and orientation of fibres in the fibre reinforced self-compacting concrete during the casting process is an important matter as the final orientation and distribution of fibres can significantly influence mechanical properties of the structural elements. A two-way coupled model for flow of suspension of rigid solid particles in a non-Newtonian fluid with a free surface has been developed for such a purpose and is shortly presented in this paper. Several experiments using an apparent yield stress fluid, i.e. Carbopol® Ultrez 21 Polymer transparent gel, were conducted and analysed by means of digital image analysis. Orientation tensor fields coming from the digital image analysis were compared with the simulation to verify the ability of the model to properly represent the flow of the fibre reinforced self-compacting concrete.*

1 INTRODUCTION

Knowledge of the final orientation and distribution of fibres is an important component in a proper understanding of the behaviour of cast structural elements. Self-compacting concrete is unfortunately not transparent which makes the experimental determination of the fibre orientation and distribution difficult. One approach in the determination of the fibre orientation might be to cast the structural element and retrieve a 3D image of the fibres using a CT scanning device [15]. Another approach might be to cast the element, cut it into sections and visually count the number of fibres at the cross-section [11]. In this paper, we present yet another approach where we, similarly to [2], substituted the self-compacting concrete by suspension of fibres in transparent Carbopol Ultrez 21 Polymer (from now on called Carbopol) allowing a direct observation of fibres.

Experimental determination of the orientation and dispersion of fibres in the self-compacting concrete is a time and resource consuming procedure. A model capable of properly simulating the given problem is therefore desired. We have developed such a model and briefly introduce it in this paper. Finally we compare the resulting fibre orientation fields coming from the experiment with the fibre orientation fields coming from the simulation model. The orientation fields of fibres are represented by second order orientation tensor fields [1].

2 METHODS

In this section, we present the two-ways coupled model for the flow of suspensions of rigid solid particles in non-Newtonian fluid. The model consists of the fluid dynamics part used to predict the free surface flow of a homogeneous fluid solved using the Lattice Boltzmann method [12, 16]. The other part of the model predicts the time and space evolution of the solid particle suspension where dynamics of the solid particles is solved using Newton's classical equations of motion. Mutual interactions between the fluid and the solid particles are represented by means of the Immersed Boundary Method with direct forcing [4].

Due to the diversity of the individual methods, the overall model is separated into three distinct levels (Figure 1):

a) **Level of fluid:** Flow of a non-Newtonian free surface fluid is solved at this level. The Lattice Boltzmann method is used as the fluid dynamics solver whereas the Mass Tracking Algorithm describes the free surface of the flow. The Lattice Boltzmann method is spatially discretized into a square / cubic grid of Eulerian nodes[1] (see square marks in Figure 1a). This level is influenced by the interaction forces coming from the "Level of fluid - solid particles interaction".

b) **Level of fluid – solid particles interaction:** This intermediate level provides a communication channel between the "Level of fluid" and the "Level of solid particles". The communication takes place via force interactions. We have used the Immersed boundary method with direct forcing to accommodate the communication between the two levels. Solid particles are discretized by a set of Lagrangian nodes[2] at this level (see black circle marks in Figure 1b). No-slip boundary condition between the fluid and the solid particles is enforced at those Lagrangian nodes. To satisfy this condition, an interaction force is created and sent back to the "Level of fluid" and the "Level of solid particles".

c) **Level of solid particles:** Solid particles with an exact analytical geometry are used at this level (see Figure 1c). The dynamics of the solid particles is solved using Newton's equations of motion. Interactions among the solid particles and between the solid particles and the boundaries (such as walls etc.) are also solved at this level. A coefficient of restitution has been incorporated to account for elastic to plastic collisions and a Coulomb friction scheme to approximate the friction. Another force, which is applied onto the solid particles, comes from the "Level of fluid - solid particles interaction" to account for the interaction between the fluid and the solid particles.

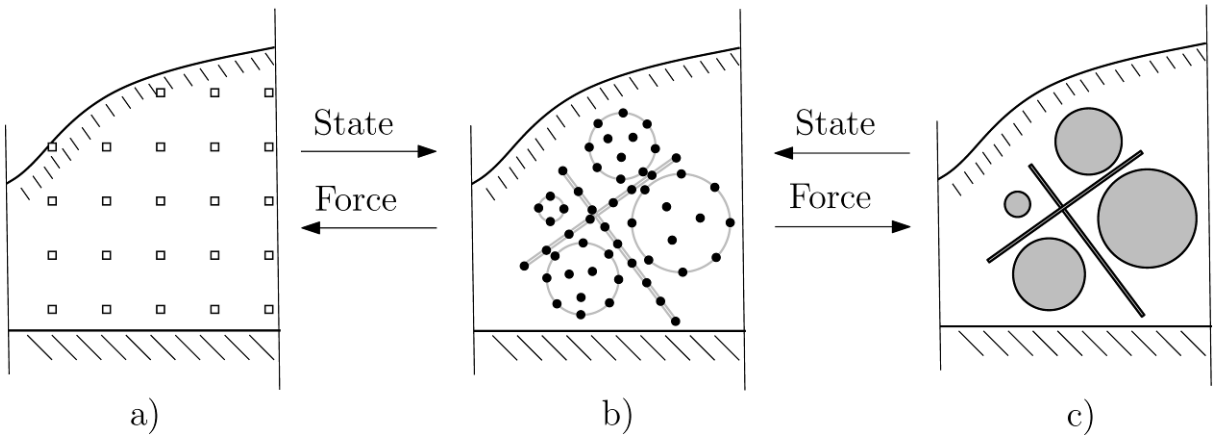

Figure 1: Scheme of the model. a) Level of fluid. b) Level of fluid – solid particles interaction. c) Level of solid particles.

3 LEVEL OF FLUID

Level of fluid solves the flow of a homogeneous non-Newtonian free surface fluid, such as the self-compacting concrete and thus consists of the fluid dynamics and free surface solver.

[1] Nodes fixed in space
[2] Position of the nodes evolves in time

3.1 Fluid Dynamics Solver

In contrast to the traditional computational fluid dynamics methods, where the problem is formulated by means of macroscopic quantities such as space and time dependent velocity and pressure fields, the Lattice Boltzmann method, with its roots in the kinetic theory of gases, treats the fluid as clouds of microscopic particles (e.g. molecules). Individual microscopic particles are assumed to be freely propagating through the space while instantaneously colliding among each other from time to time (see Lattice gas cellular automata [16]). The clouds of particles are approximated by continuous particle distribution functions (i.e. probability of a particle occurrence). The particle distribution functions are further discretized by a set of discrete particle distributions to limit the number of unknowns. Lattice Boltzmann equation provides rules for mutual collisions and propagation of the particle distributions. The macroscopic quantities (density, velocity et.) can then be computed as moments of the particle distributions.

The computational domain is typically discretized by a set of Eulerian cells of a uniform size (see Figure 1a). Continuous fields of macroscopic quantities (such as velocity fields) are then approximated by the mean values of the quantities in the discretized cells. Similarly, the time is discretized into uniform time steps.

In a given time step, the state of the fluid in a cell is fully described by the particle distributions in that cell. The particle distributions in the given time step at a certain position are computed from the particle distributions in neighbouring cells in the previous step. This accounts for the propagation of the particle distributions. Collisions of the particle distributions are in the simplest case approximated by a linear transformation of the particle distributions towards the local equilibrium state. Such a transformation is called Bhatnagar-Gross-Krook collision operator [3]. The local equilibrium state is based on the Maxwell-Boltzmann distribution, and is computed from the local macroscopic velocity and pressure (density) of the fluid. The difference between the current state of the particle distributions and the local equilibrium state allows for a simple approximation of the local shear rate and shear stress tensors [9].

3.2 Free surface algorithm

A free surface has been implemented in the form of the Mass Tracking Algorithm [6]. The algorithm makes use of the same Eulerian discretized domain as the Lattice Boltzmann method where fluid, gas and interface cells are introduced. The Lattice Boltzmann equation is computed in the fluid and interface cells, only. Gas cells are empty cells where nothing is computed. Interface cells separate fluid phase and gas phase and are therefore responsible for a correct implementation of the free surface algorithm and for the correct mass conservation of the fluid. Interface cells are moreover the only place where the Mass Tracking Algorithm comes into play in the form of local mass tracking and reconstruction of missing information from the gas phase.

3.3 Level of fluid - solid particles interaction

The Immersed boundary method with direct forcing [4] provides a direct linkage between the “Level of fluid” and the “Level of solid particles”. The fluid can “feel” the solid particles in the form of a force field. In the same manner, the solid particles can “feel” the fluid in the form of forces acting on the solid particles. At this level, the solid particles are discretized into a set of Lagrangian nodes. It is assumed that the velocity of a solid particle and the fluid at the same Lagrangian node are equal due to the no-slip boundary condition. Non-equal velocities are transformed into a force field acting on both the particle and the fluid. The force is in the simplest form computed based on Newton's second law of motion (i.e. such a force to accelerate a certain volume of the fluid that is surrounding the Lagrangian node to the velocity of the solid particle at that Lagrangian node). Since the Lagrangian nodes do not coincide with the Eulerian nodes coming from the “Level of fluid”, the velocity of the fluid in the Lagrangian nodes is obtained by a volume averaging of the velocities at the Eulerian nodes. The volume averaging is conducted by means of a Dirac delta function [17]. The resulting forces are

usually extrapolated from the Lagrangian nodes back to the Eulerian nodes (i.e. to the “Level of fluid”) using the same Dirac delta function.

The Immersed Boundary Method provides, contrary to other methods (eg. bounce-back wall scheme [7, 8]), smooth and stable time evolution of all the quantities (i.e. the position of the solid particles or forces acting on them). The most important feature of the Immersed Boundary Method, however, is its ability to simulate small objects of only a few lattice units or even sub-grid sized objects, see [14]. This results in a significant reduction of the computational time needed.

3.4 Level of solid particles

At this level, the solid particles are assumed to be rigid bodies of a simple geometric shape (sphere, ellipsoid or cylinder) with the ability to move, rotate and interact among each other, with fluid, walls and other obstacles. The dynamics of those immersed solid particles is driven by Newton's second law of motion which is discretized with the explicit Runge-Kutta-Fehlberg time integration scheme with an adaptive time step. The numerical integration scheme that we adopted ensures the stability and accuracy of the simulation even for a highly non-linear behaviour.

An accurate and robust treatment of interactions among the solid particles and between the solid particles and other obstacles such as walls or reinforcement plays an important role in a proper description of the relevant phenomena. The model includes two types of interactions, namely mutual instantaneous collisions of solid particles and continuous forcing of a general type. The instantaneous collisions were approximated by means of force impulses [13]. An example of the continuous forcing could be a lubrication force correcting the fluid flow between two solid particles in the case when the two solid particles approach each other to a sub-grid distance [10].

4 APPLICATIONS

Verification of a newly developed model is a crucial part of its development phase. We presented a full description of our model and its basic verification in [13]. A comparison of the model with a real-world casting of a fibre reinforced self-compacting concrete plate was given in [15]. In this paper, we aim to compare the presented model with an L-Box experiment with the use of a transparent yield stress fluid, Carbopol.

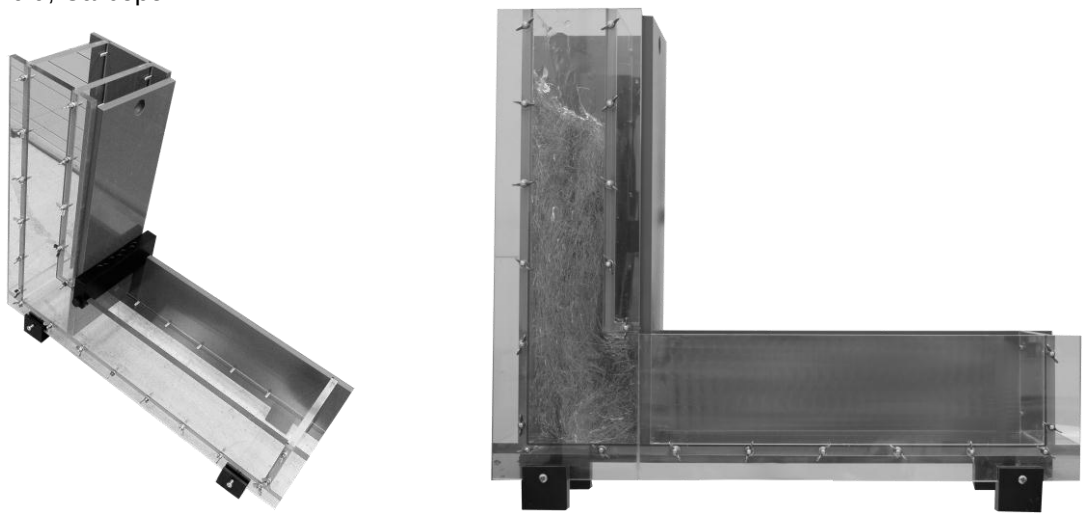

Figure 2: Transparent L-Box form (see Section 4.2 for the dimensions and other parameters)

4.1 Transparent L-Box experiment

In this experiment, we cast a suspension of stainless steel fibres in Carbopol into a formwork and visually study how the fibres orient and disperse due to the flow. We have chosen the L-Box form as a primary formwork of the study. Figure 2 shows the shape of the transparent plastic standard-sized L-Box both in the emptied and filled state.

As mentioned, we have used a gel-like fluid Carbopol which is a transparent shear thinning polymer with an apparent yield stress. It can further be assumed to follow a Bingham rheology model for shear rates between 0 and 5 s^{-1} [5]. The two features, i.e. transparency and Bingham rheology, make Carbopol a suitable substitute for the fluid matrix in self-compacting concrete. Carbopol has, compared to the self-compacting concrete, a relatively low pH (ca. 6.5). We have therefore used stainless steel fibres Dramix rl 80/30sn produced by Bekaert Belgium to avoid any corrosion of the suspended fibres.

The Carbopol was produced according to the guidelines of the Lubrizol Company. We did not, however, succeed to avoid the creation of a large amount of air voids in the fluid. A desiccator was therefore used to produce a high under-pressure and thus to boil the air voids out of the fluid. We produced two different batches of the Carbopol fluid. One with the 0.125 volume percentage of Carbopol, the other one with double the amount of Carbopol in the fluid.

The resulting mean values of the plastic viscosity and the yield stress of the two batches were measured by Advanced Rheometer 2000 produced by TA Instruments, and read 5 Pa.s, 8 Pa and 15 Pa.s, 30 Pa, respectively. Although different values of the Bingham parameters were reached, the final shapes of the orientation ellipses of the fibres were very similar. We therefore present results of the first batch only.

Each casting was done three times to account for the natural variance in results. Photographs of the final state of the three castings together with the orientation ellipses of the fibres are shown in Figure 3.

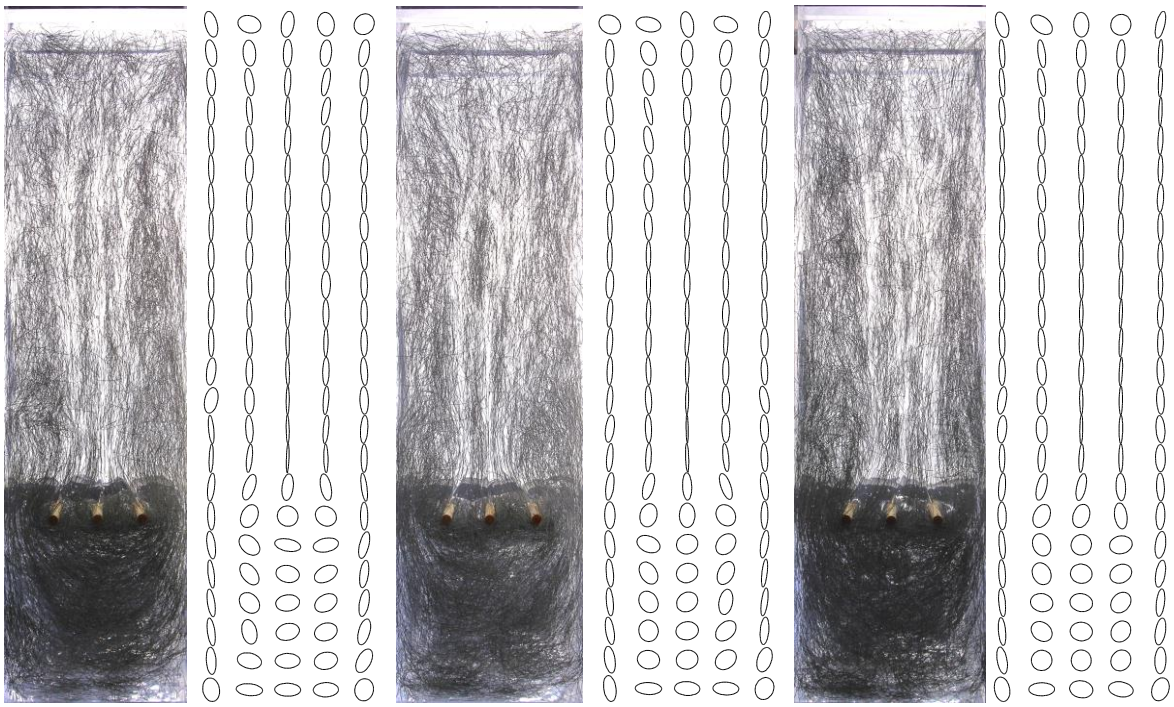

Figure 3: Top view photographs of the final state of 3 experiments and their orientation ellipses.

The orientation ellipses of the fibres serve as a visual representation of the second order orientation tensors as described in [1]. The thinner the ellipses the more oriented fibres occur in the region. Vice versa, the circular ellipses stand for a random orientation of the fibres in the region.

To obtain the orientation ellipses, we took high resolution photographs of the final state of the flow (see Figure 3). The photographs were then transformed by Bradley local thresholding, adaptive smoothing and simple skeletonization technique to obtain a binary image (see AForge.NET framework). The binary image was then converted into the second order orientation tensors as described in [5] and visualized by orientation ellipses.

As can be seen in Figure 3, there are regions which are very complicated to analyse due to either spurious elements (eg. horizontal bar in the upper part of the figure), decreased transparency of the form due to reinforcement mounting or due to high fibre volume concentrations. Resulting orientation ellipses should therefore be treated with caution, especially when compared to the ideal situation in the case of numerical simulations.

4.2 L-Box simulation

An L-Box simulation was run and the results of the simulation were compared to the experimental results. The initial and boundary conditions of the simulation were as follows. The height, length and the width of the L-Box were 0.6 x 0.7 x 0.2 m. Three reinforcing bars of the diameter of 9 mm were placed into the L-Box. Spacing of the bars was 62 mm, 38 mm, 38 mm and 62 mm. The density, plastic viscosity and the yield stress of the fluid were set to 950 kg/m^3, 5 Pa.s and 8 Pa. A total amount of 0.5 % volume fraction of the fibres was used in the simulation. Straight fibres of the length 6 cm, aspect ratio 80 and density 7500 kg/m^3 were used. All the collisions of the fibres with the surrounding (fibres, walls, reinforcing bars) were assumed to be plastic, i.e. the coefficient of restitution was set to 0. Friction of the fibres was assumed to follow Coulomb friction model with the dynamic and static friction coefficient set to 0.3. The domain was spatially discretized by 1 cm = 3 lattice units. The fibre length was therefore 18 lattice units and the diameter was 0.225 lattice units. A correction term as described in [14] was applied to adjust the force fields in the Immersed boundary methoddue to the sub-grid diameter of the fibres.

A 3D view of the initial state, the top view of the final state and the top view of the orientation ellipses of the final state are presented in Figure 4.

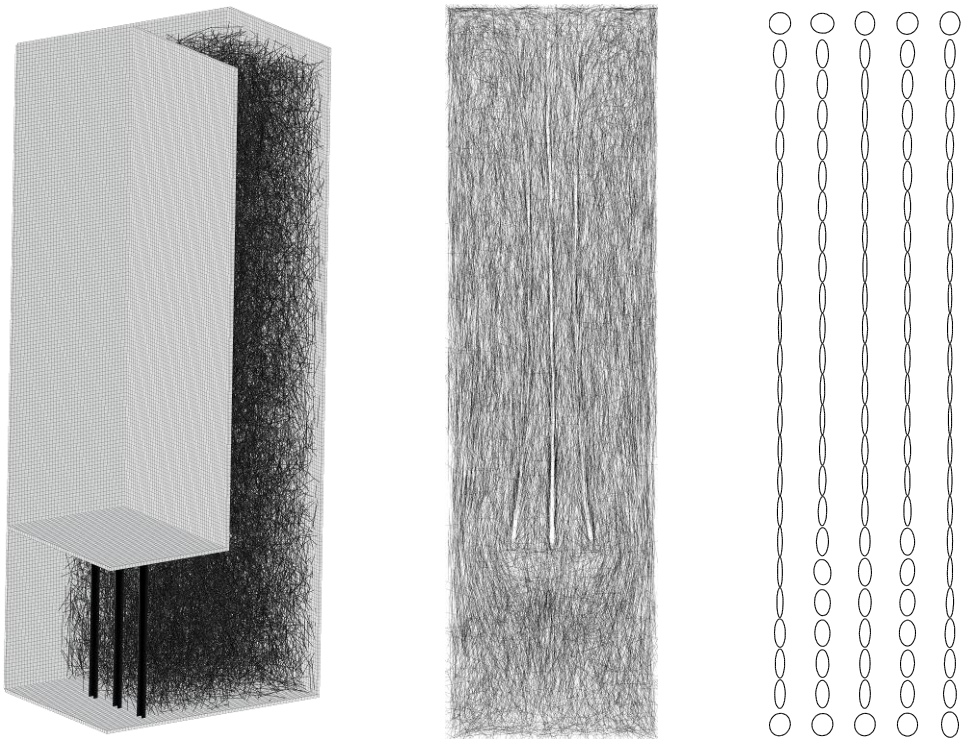

Figure 4: 3D section of the initial state of the simulation; Top view of the final state of the simulation and its orientation ellipses

Approximately 5 seconds of flow was simulated corresponding to ca. 20 000 time steps. The number of fibres in the simulation was 21734. The simulation took ca. 20 days on a single core 2 GHz CPU. Two thirds of the computation time was consumed by the “Level of solid particles” and the “Level of fluid – solid particles interaction”. One third of the computation time was consumed by the “Level of fluid”.

5 RESULTS AND DISCUSSION

We have developed a computational model capable of simulating a suspension of aggregates and fibres in the non-Newtonian free surface fluid. The model has recently been parallelized and is therefore presently capable of simulating ca. 100 000 particles in a reasonable amount of time based on the computational power available. This makes the micro-, meso- up to macro-scale simulations possible.

We have conducted an experimental work with a transparent yield stress fluid, Carbopol, and analysed the final states of the fibre orientation by means of orientation ellipses.

The comparison of the orientation ellipses coming from the experimental work and coming from the simulation indicates the ability of our model to correctly predict the final orientation of fibres in the fibre reinforced self-compacting concrete.

6 ACKNOWLEDGEMENTS

We thank E. M. Hvilsom and G. D. Rasmussen for their important contribution during the experimental work.

The first author acknowledges funding from the Danish Agency for Science Technology and Innovation, “Sustainable Concrete Structures with Steel Fibres - The SFRC Consortium” Grant no. 09-069955.

The second author acknowledges funding from the Danish Agency for Science Technology and Innovation (project 09-065049/FTP: Prediction of flow induced inhomogeneities in self-compacting concrete).

REFERENCES

[1] Advani, S.G. 1987. The Use of Tensors to Describe and Predict Fiber Orientation in Short Fiber Composites. *Journal of Rheology*. 31, 8 (1987), 751.

[2] Boulekbache, B. et al. 2010. Flowability of fibre-reinforced concrete and its effect on the mechanical properties of the material. *Construction and Building Materials*. 24, 9 (Sep. 2010), 1664-1671.

[3] Chen, S. and Doolen, G.D. 1998. Lattice Boltzmann method for fluid flows. *Annual Review of Fluid Mechanics*. 30, 1 (Jan. 1998), 329-364.

[4] Feng, Z. and Michaelides, E. 2005. Proteus: a direct forcing method in the simulations of particulate flows. *Journal of Computational Physics*. 202, 1 (Jan. 2005), 20-51.

[5] Hvilsom, E.M. and Rasmussen, G.D. 2011. *Fibre Orientation and Distribution in Steel Fibre Reinforced SCC*. Technical University of Denmark.

[6] Körner, C. et al. 2005. Lattice Boltzmann Model for Free Surface Flow for Modeling Foaming. *Journal of Statistical Physics*. 121, 1-2 (Oct. 2005), 179-196.

[7] Ladd, A. 1994. Numerical simulations of particulate suspensions via a discretized Boltzmann equation. Part 1. Theoretical foundation. *Journal of Fluid Mechanics*. 211, (1994).

[8] Ladd, A.J.C. 1994. Numerical simulations of particulate suspensions via a discretized Boltzmann equation. Part 2. Numerical results. *Journal of Fluid Mechanics*. 271, 1 (1994), 311–339.

[9] Mei, R. et al. 2002. Force evaluation in the lattice Boltzmann method involving curved geometry. *Physical Review E*. 65, 4 (Apr. 2002), 1-14.

[10] Nguyen, N.-Q. and Ladd, A. 2002. Lubrication corrections for lattice-Boltzmann simulations of particle suspensions. *Physical Review E*. 66, 4 (Oct. 2002), 1-12.

[11] Sarmiento, E.V. 2011. *Influence of concrete flow on the mechanical properties of ordinary and fibre reinforced concrete*. Technical University of Catalonia.

[12] Sukop, M.C. and Thorne, D.T. 2005. *Lattice Boltzmann Modeling: An Introduction for Geoscientists and Engineers*. Springer.

[13] Svec, O. and Skocek, J. 2012. Model predicting the flow of a suspension of rigid solid particles in a non-Newtonian fluid. *To be published*. (2012).

[14] Svec, O. et al. 2011. Flow simulation of fiber reinforced self compacting concrete using Lattice Boltzmann method. *Proceedings of ICCC* (2011).

[15] Svec, O. et al. 2012. Application of the fluid dynamics model to the field of fibre reinforced self-compacting concrete. *Proceedings of SSCS* (2012).

[16] Wolf-Gladrow, D.A. 2000. *Lattice-Gas Cellular Automata and Lattice Boltzmann Models: An Introduction (Lecture Notes in Mathematics)*. Springer.

[17] Yang, X. et al. 2009. A smoothing technique for discrete delta functions with application to immersed boundary method in moving boundary simulations. *Journal of Computational Physics*. 228, 20 (Nov. 2009), 7821-7836.